

Proceeding Paper

# Synthesis and Characterization of Graphene-Oxide Reinforced Copper Matrix Composite <sup>†</sup>

Isaque Alan de Brito Moura <sup>\*</sup>, Talita Gama de Sousa, Andreza Menezes Lima, Wesley Oliveira da Silva and Luiz Paulo Brandao

Military Institute of Engineering (IME), Department of Materials Science—SE/8, Praça General Tibúrcio, 80, Urca, Rio de Janeiro, RJ 22290-270, Brazil; talitagama@ime.eb.br (T.G.d.S.); andrezamenezeslima@gmail.com (A.M.L.); oliveira.dje@gmail.com (W.O.d.S.); brandao@ime.eb.br (L.P.B.)

<sup>\*</sup> Correspondence: isaquebrito@ime.eb.br

<sup>†</sup> Presented at the 2nd International Online-Conference on Nanomaterials, 15–30 November 2020;

Available online: <https://iocn2020.sciforum.net/>.

**Abstract:** In this study, eletrolitical copper powder (Cu) was initially mixed with the aqueous solution of graphene oxide (GO); later, the mixture underwent mechanical stirring for 1 h, vacuum filtration, and drying for 42 h. The final concentration of GO in the composite was 0.3%wt. Through scanning electron microscopy (SEM), it was possible to observe the homogeneous dispersion of graphene sheets between copper particles, without the presence of agglomerates. In addition, X-ray diffraction (XRD) of the pure samples and after mixing revealed that there was no oxidation of the copper and the absence of peaks related to other elements, confirming the high purity of the copper used. Still, by XRD, it was possible to analyze that the graphene oxide produced was formed by stacking layers of graphene owing to the appearance of a diffraction peak referring to the plane (002), which was confirmed by Raman spectroscopy performed in GO from the appearance of the 2D bands. Fourier transform infrared spectroscopy (FTIR) allowed the identification of the vibrational spectra referring to the hydroxyl, carbonyl, and epoxy functional groups in GO, confirming that the oxidation process was effective in inserting functional groups in the basal graphical plane. Through the GO thermogravimetric analysis (TGA), it was possible to identify a significant loss of mass of approximately 30% at temperatures below 100 °C; referring to the elimination of water molecules, the most stable functional groups were eliminated at temperatures between 600 °C and 800 °C.

**Citation:** Moura, I.A.B.; Sousa, T.G.; Lima, A.M.; Oliveira, W.S.; Brandao, L.P. Synthesis and Characterization of Graphene-Oxide Reinforced Copper Matrix Composite. *Mater. Proc.* **2021**, *4*, 72. <https://doi.org/10.3390/IOC2020-08000>

Academic Editors: Ana María Díez-Pascual, Antonio Di Bartolomeo and Guanying Chen

**Keywords:** graphene oxide; copper; TGA; FTIR; SEM

Published: 15 November 2020

**Publisher's Note:** MDPI stays neutral with regard to jurisdictional claims in published maps and institutional affiliations.



**Copyright:** © 2020 by the authors. Licensee MDPI, Basel, Switzerland. This article is an open access article distributed under the terms and conditions of the Creative Commons Attribution (CC BY) license (<http://creativecommons.org/licenses/by/4.0/>).

## 1. Introduction

The interest in the study and development of routes to increase copper resistance has received special attention from researchers in recent years [1,2], especially the formation of composites with different types of addition of reinforcement material. This is owing to this method having been effective in improving its mechanical properties, interfering less significantly in the electrical conductivity [3–6]. In this prerogative, carbon-based materials, when used as reinforcements, increase the strength of the matrix without much compromising the electrical conductivity of the composite [7]. One of the factors that explains this characteristic is the low solubility between copper and carbon, making the diffusion of the carbonaceous material in the copper matrix very low [7,8]. Thanks to its superior characteristics to other materials, graphene and its derivatives have been studied for incorporation into these composites, showing high values of mechanical resistance and electrical conductivity. Graphene is a planar carbon monolayer whose atoms are arranged in two-dimensional form (2D) and is considered the most resistant material ever tested, obtaining tensile strength values of 130 GPa [9,10]. In addition, it has high values

of electrical ( $\sigma = 10^6 \text{ } \Omega\text{cm}^{-1}$ ) and thermal conductivity ( $5000 \text{ Wm}^{-1} \text{ K}^{-1}$ ) [11,12]. Graphene oxide (GO) is the main derivative of graphene and its structure contains many oxygen-containing functional groups, e.g., epoxy, hydroxyls, carbonyls, and carboxyls linked to the layer of carbon atoms [13]. The manufacture of copper-graphene composites has been studied through the use of several manufacturing techniques and different attempts to determine processing parameters. Among them are the obtaining of an optimized dispersion of graphene in the matrix, favoring a good adhesion between the components, and an attempt to minimize the agglomeration of graphene between grain boundaries; the latter has been one of the greatest challenges [14–16]. The analysis of powders is essential because of the need to understand the changes that materials can undergo in their properties when performing different processes [17]. For a better understanding of the final properties of the composite in this study, thermal and microstructural analysis of Cu-Gr powders was performed, presented in a systematic manner below.

## 2. Materials and Methods

### 2.1. Preparation of Cu/GO Composite

The GO used in this study was produced by liquid-phase exfoliation (LPE), based on the method of Hummers and Offeman (1958) [18], and modified by Rourke et al. (2011) [19]. This method allows to obtain GO sheets with a great superficial extension and a large amount of oxidized functional groups, which in turn facilitate the adhesion of nanoparticulate materials on its surface. Pure copper powder (Cu) with a purity of 99.94% and graphene oxide with a concentration of 4.55 mg/mL were mixed by mechanical stirring for 1 h. The chemical composition of the composite was 0.3%wt GO. Vacuum filtration using kitassato and Buncher funnel was performed followed by vacuum drying for 42 h in order to obtain the dry powder.

### 2.2. Characterization

The morphologies of copper and Cu/GO composite powders were observed by scanning electron microscopy (SEM, FEI Quanta FEG 250). X-ray diffraction (XRD, PANalytical X Pert Pro MRD) was performed with  $\text{Co K}\alpha$  radiation and operated at 40 kV and 40 mA. Raman spectra (NT-MDT NTEGRA Spectra) was performed on GO in order to observe the bands D and G; the wavelength of the laser used was 473 nm with a scanning range between 702 and 3343  $\text{cm}^{-1}$ , and an exposure time of 200 s. Thermogravimetric analysis (TGA, TGA Q-500 equipment) and Fourier transform infrared (FTIR, Perkin Elmer FT-IR/FIR spectrometer with ATR accessory) were performed on GO and Cu/GO composites; for TGA analyses, the samples were analyzed up to 800 °C, in a controlled atmosphere of nitrogen, with a heating rate of 10 °C/min, and FTIR was taken with a number of scans of 60 and 4  $\text{cm}^{-1}$  resolution.

## 3. Results and Discussion

### 3.1. Powders and GO Morphology and Microstructural Analysis

In Figure 1a,b, SEM images of the pure copper powder are presented; the granulometric distribution has a wide range and, in general, it can be seen that the particles have an irregular shape, being constituted by clusters of smaller particles, as is possible to note, specifically, in the image of Figure 1b. The particle shape and sizes are consistent with the electrolytic manufacturing process used, which gives rise to irregular or dendritic particles with an average particle size between 5 and 300 nm calculated by Faria et al. [20]. In Figure 1c,d, the images of the copper-graphene composite are presented, in which the particles resemble the aspect of the pure copper powder, presented in Figure 1a. It is possible to identify the GO sheets adhered to the surface of the copper particles and between the particles, showing adhesion between the copper and the GO.

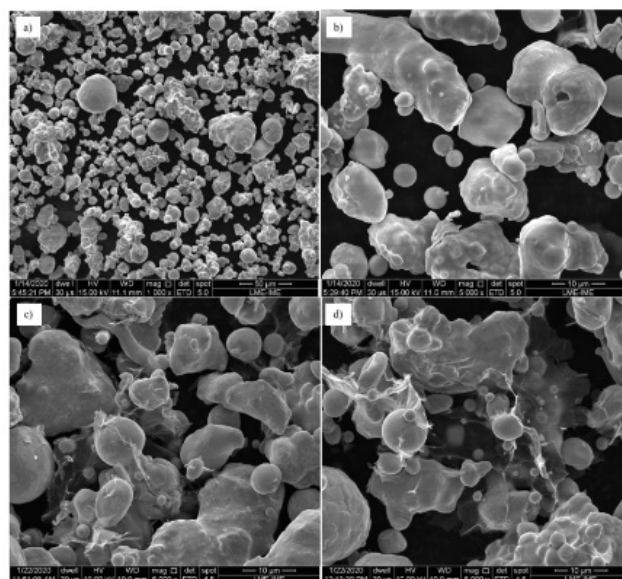


**Figure 1.** Scanning electron microscopy (SEM): (a,b) pure copper and (c,d) composite Cu/graphene oxide (GO).

Figure 2a shows the diffractogram obtained for graphene oxide. Through the synthesis used, we have the generation of few layers of graphene, with it being possible to obtain a sharp diffraction peak in the diffractogram start. The identified peak refers to plane (002), related to the HC structure of carbon. The diffraction peaks shown in the diffractogram refer to the leaves that are not arranged in the form of monolayers, as monolayers do not show a diffraction peak. Thus, together with the production method, there is an indication that the GO used for this study is formed by several layers. In Figure 2a, one can notice a decrease in the diffraction angle in relation to pure graphite, used for GO production, attributed to the increase in GO interplanar distances due to the insertion of functional groups during oxidation and the possibility of the presence of water molecules between the layers [21]. Figure 2b shows the diffractogram obtained for the pure copper powder and for composite Cu/GO, with the peaks referring to planes (111), (200), (220), (311), and (222). These plans refer to the FCC structure of copper and no other peak was indexed, ensuring that the copper powder did not have other elements or oxidation, or the present oxidation resulted in a very small amount of oxide, being insufficient to generate a peak above the noise of the diffractogram. In addition, no peak was observed for the GO, owing to the concentration used to manufacture the composite being so low that it does not generate a diffraction peak.

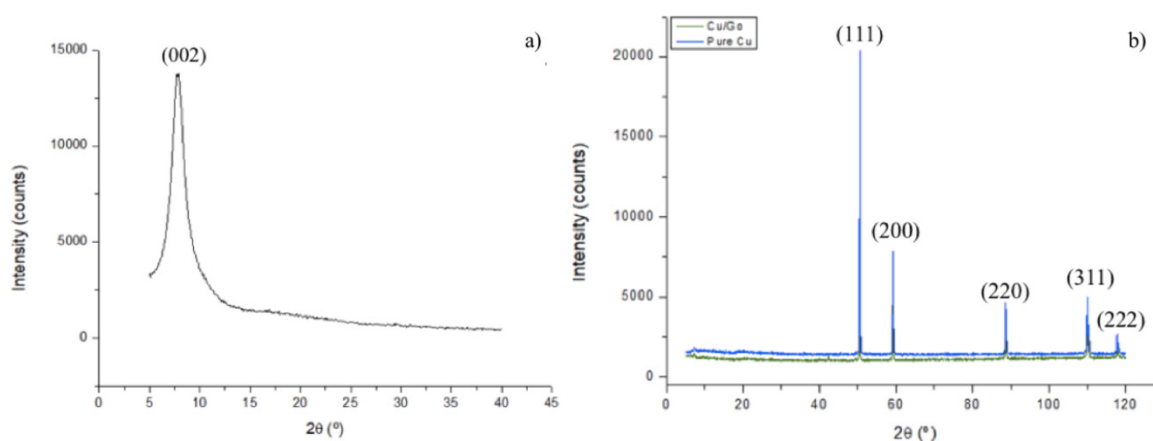


**Figure 2.** X-ray diffraction (XRD) of (a) GO and (b) pure copper and Cu/GO composite.

### 3.2. Spectroscopy

#### 3.2.1. Raman Analysis

Raman spectroscopy was performed on the dispersion of graphene oxide used for the manufacture of the powdered composite. Figure 3 presents the Raman spectra found for the GO.

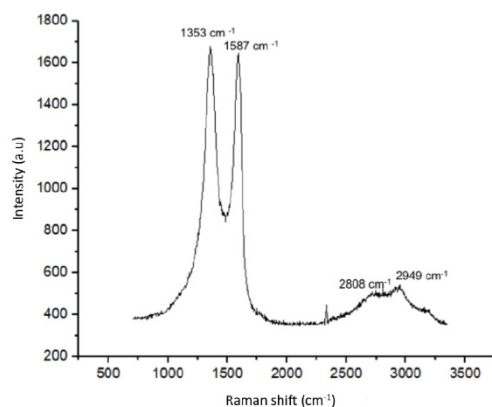


**Figure 3.** Raman spectra of GO used.

The Raman spectra of graphene normally shows peaks referring to the D ( $\sim 1350\text{ cm}^{-1}$ ) and G ( $\sim 1580\text{ cm}^{-1}$ ) bands. In this study, bands D ( $1353\text{ cm}^{-1}$ ) and G ( $1587\text{ cm}^{-1}$ ) with Raman displacement, similar to those found in the works of Faria et al. [20], Yue et al. [22], and Gao et al. [23], were found. The relationship between the intensities of bands D and G allows to obtain the amount of defects present in the carbon structure. The ID/IG ratio for GO is greater than that of graphene and reduced graphene oxide, and this is owing to the presence of oxygenated functional groups linked to the carbon structure [15]. The ratio of the intensities of bands D and G used in this study was approximately 1.0. In addition to the bands D and G, it was possible to observe the presence of the peaks referring to the bands 2D ( $2808\text{ cm}^{-1}$ ) and 2D' ( $2949\text{ cm}^{-1}$ ). These bands appear with less intensity in relation to the D and G bands and are related to the stacking of a number of carbon layers of the graphene structure [24]. Thus, the presence of these bands shows that the oxide analyzed is formed by stacking layers and not just monolayers, which can be confirmed by the X-ray diffraction analysis presented in Figure 2a.

#### 3.2.2. Fourier Transform Infrared Spectroscopy

Fourier transform infrared spectroscopy (FTIR) was obtained at the Instrumental Support Laboratory (LAPIN1) of the Institute of Macromolecules Professora Eloisa Mano (IMA-UFRJ). The analysis of the spectrum obtained for GO (Figure 4a) allows us to initially observe the occurrence of a broadband between  $3000$  to  $3700\text{ cm}^{-1}$ , which is related to the existence of water adsorbed between the leaves and a peak at  $3347\text{ cm}^{-1}$ , which can be attributed to the OH stretching range. At  $1626\text{ cm}^{-1}$ , another peak is identified, corresponding to the stretching vibrations of C=O, followed by a third peak at  $1158\text{ cm}^{-1}$ , referring to vibrations of C-O-C epoxy groups; at  $1036\text{ cm}^{-1}$ , vibrations of C-OH bonds and, finally, a last peak at  $873\text{ cm}^{-1}$  due to the stretching vibrations of epoxy groups [25–27]. For composite Cu/GO, presented in Figure 4b, some characteristic peaks can be observed relative to the GO, presented in Figure 4a, such as the existence of a band present at approximately  $3500\text{ cm}^{-1}$ , related to the O-H elongation vibration. The absorption bands observed at  $2954\text{ cm}^{-1}$  can correspond to symmetric vibration of C-H bond. At  $1060\text{ cm}^{-1}$ , a band related to C-O elongation (epoxy/ether) is noted. A peak appeared at  $596\text{ cm}^{-1}$ , which is attributed to observation of hydroxyl deformation modes [15,28,29].

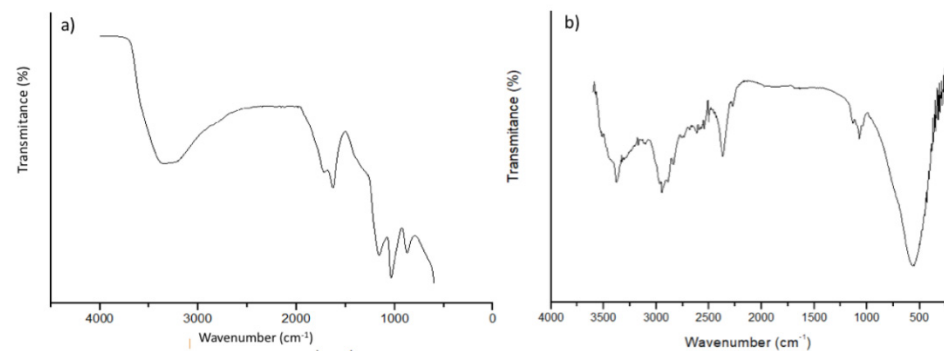


**Figure 4.** Fourier transform infrared spectroscopy (FTIR) spectra of (a) GO and (b) Cu/GO composite.

### 3.3. Thermogravimetric Analysis

Thermal analysis was performed on GO and composite powder in order to verify the effectiveness of the method of mechanical stirring, filtration, and vacuum drying. The thermogravimetric analysis (TGA) is seen in Figure 5, and was also obtained at LAPIN1 (IMA-UFRJ).

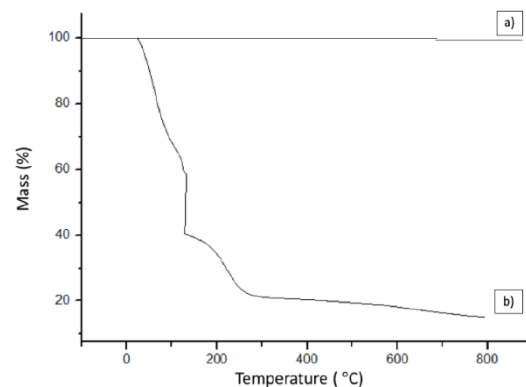


**Figure 5.** Thermogravimetric analysis (TGA) of (a) Cu/GO composite and (b) GO.

For the composite (Figure 5a), it is possible to notice that there is no change in mass; as there was no gain, it is possible to deduce that there was no oxidation; and the fact that there is no loss of weight is due to the low amount of graphene in the composite, being formed mainly of copper [30]. For GO (Figure 5b), it is possible to initially observe a loss of mass below 100 °C, of about 30%, which is associated with the elimination of adsorbed water and gas molecules. The range between 100 and 200 °C shows an abrupt loss of 34% in mass and, between 200 and 300 °C, of 13%, which are related to the elimination of functional oxygen groups. In the region of 300–600 °C, the material remains stable, showing a small loss of mass (approximately 3%), followed by a last loss in the region of 600–800 °C, related to the removal of functional oxygen groups being even more stable [25,26].

## 4. Conclusions

In conclusion, copper–graphene composites were synthesized by mechanical stirring. Based on the results obtained by SEM and XRD, it is suggested that uniform mixtures of GO between the copper particles were obtained such that there were no large agglomerates, showing that the mixing method through the mechanical stirring of the powder in aqueous dispersion was efficient to obtain the composite powder with good homogeneity and no oxidation. The GO used was formed by several layers, which was confirmed by the presence of 2D bands in Raman spectra.

**Author Contributions:** Conceptualization, I.A.d.B.M. and T.G.d.S.; methodology, I.A.d.B.M.; software, A.M.L.; validation, L.P.B. and T.G.d.S.; formal analysis, I.A.d.B.M.; investigation, I.A.d.B.M.; data curation, I.A.d.B.M., T.G.d.S., A.M.L. and W.O.d.S.; writing—original draft preparation, I.A.d.B.M.; writing—review and editing, T.G.d.S., A.M.L., W.O.d.S. and L.P.B.; visualization, L.P.B.; supervision, L.P.B.; project administration, T.G.d.S. All authors have read and agreed to the published version of the manuscript. Version 9 November 2020 submitted to Journal Not Specified 6 of 7. All authors have read and agreed to the published version of the manuscript.

**Acknowledgments:** The authors thank the Brazilian supporting agencies FAPERJ and CNPq for the funding; the Military Institute of Engineering for assistance during this research; and acknowledgements to the Federal University of Rio de Janeiro (UFRJ) and Pontifical Catholic University (PUC) for the support in the spectroscopy and thermal analysis.

**Conflicts of Interest:** The authors declare no conflict of interest.

## References

1. Sousa, T.G.; Moura, I.A.B.; Filho, F.C.G.; Monteiro, S.N.; Brandão, L.P. Combining severe plastic deformation and precipitation to enhance mechanical strength and electrical conductivity of Cu–0.65Cr–0.08Zr alloy. *J. Mater. Res. Technol.* **2020**, *9*, 5953–5961.
2. Meng, A.; Nie, J.; Wei, K.; Kang, H.; Liu, Z.; Zhao, Y. Optimization of strength, ductility and electrical conductivity of a Cu–Cr–Zr alloy by cold rolling and aging treatment. *Vacuum* **2019**, *167*, 329–335.
3. Wang, J.; Guo, L.; Lin, W.; Chen, J.; Zhang, S.; Chen, S.; Zhen, T.; Zhang, Y. The effects of graphene content on the corrosion resistance, and electrical, thermal and mechanical properties of graphene/copper composites. *New Carbon Mater.* **2019**, *787*, 786–793.
4. Moghanian, A.; Sharifianjazi, F.; Abachi, P.; Sadeghi, E.; Jafarikhorami, H.; Sedghi, A. Production and properties of Cu/TiO<sub>2</sub> nano-composites. *J. Alloys Compd.* **2017**, *698*, 518–524.
5. Selvakumar, V.; Muruganandam, S.; Senthilkumar, N. Evaluation of mechanical and tribological behavior of Al-4%Cu-x%SiC composites prepared through powder metallurgy technique. *Trans. Indian Inst. Met.* **2017**, *70*, 1305–1315.
6. Singh, V.; Joung, D.; Zhai, L.; Das, S.; Khondaker, S.I.; Seal, S. Graphene based material: Past, present and future. *Prog. Mater. Sci.* **2011**, *56*, 1178–1271.
7. Singh, M.; Yadav, A.; Kumar, S.; Agarwal, P. Annealing induced electrical conduction and band gap variation in thermally reduced graphene oxide films with different sp<sup>2</sup>/sp<sup>3</sup> fraction. *Appl. Surf. Sci.* **2015**, *326*, 236–242.
8. Boostani, A.F.; Tahamtan, S.; Jiang, Z.Y.; Wei, D.; Yazdani, S.; Khosroshahi, R.A.; Mousavian, R.T.; Xu, J.; Zhang, X.; Gong, D. Enhanced tensile properties of aluminium matrix composites reinforced with graphene encapsulated SiC nanoparticles. *Compos. Part A Appl. Sci. Manuf.* **2015**, *68*, 155–163.
9. Baladin, A.A.; Ghosh, S.; Bao, W.; Calizo, I.; Teweldebrhan, D.; Miao, F.; Lau, C.N. Superior thermal conductivity of single-layer graphene. *Nano Lett.* **2008**, *8*, 902–907.
10. Geim, A.K.; Novoselov, K.S. The rise of graphene. *Nat. Mater.* **2007**, *6*, 183.
11. Novoselov, K.S.; Geim, A.K.; Morozov, S.V.; Jiang, D.; Zhang, Y.; Dubonos, S.V.; Grigorieva, I.V.; Firsov, A.A. Electric field effect in atomically thin carbon films. *Science* **2004**, *306*, 666–669.
12. Novoselov, K.S.; Geim, A.K.; Morozov, S.V.; Jiang, D.; Katsnelson, M.I.; Grigorieva, I.; Dubonos, S.; Firsov, A.A. Two-dimensional gas of massless Dirac fermions in graphene. *Nature* **2005**, *438*, 197–200.
13. Gao, W.; Alemany, L.B.; Cl, L.; Ajayan, P.M. New insights into the structure and reduction of graphite oxide. *Nat. Chem.* **2009**, *1*, 403–408.
14. Jagannadham, K. Thermal conductivity of copper-graphene composite films synthesized by electrochemical deposition with exfoliated graphene platelets. *Metall. Mater. Trans.* **2011**, *43*, 316–324.
15. Hwang, J.; Yoon, T.; Jin, S.H.; Lee, J.; Kim, T.S.; Hong, S.H.; Jeon, S. Enhanced mechanical properties of graphene/copper nano-composites using a molecular-level mixing process. *Adv. Mater.* **2013**, *25*, 6724–6729.
16. Dutkiewicz, J.; Ozga, P.; Maziarz, W.; Pstruś, J.; Kania, B.; Bobrowski, P.; Stolarska, J. Microstructure and properties of bulk copper matrix composites strengthened with various kinds of graphene nanoplatelets. *Mater. Sci. Eng. A* **2015**, *628*, 124–134.
17. Tian, Y.; Cheung, H.C.; Zheng, R.; Ma, Q.; Chen, Y.; Delepine-Gilon, N.; Yu, J. Elemental analysis of powders with surface-assisted thin film laser-induced breakdown spectroscopy. *Spectrochim. Acta Part B* **2016**, *124*, 16–24.
18. Hummers, W.S.; Offeman, R.E. Preparation of Graphitic Oxide. *J. Am. Chem. Soc.* **1957**, *208*, 1937–1957.
19. Rourke, J.P.; Pandey, P.A.; Moore, J.J.; Bates, M.; Kinloch, I.A.; Young, R.J.; Wilson, N.R. The Real Graphene Oxide Revealed: Stripping the Oxidative Debris from the Graphene-like Sheets. *Angew. Chem. Int.* **2011**, *50*, 3173–3177.
20. Faria, G.S.; Lima, A.M.; Pinheiro, W.A.; Ribeiro, A.A.; Brandão, L.P.M. Compósitos cobre-grafeno produzidos por metalurgia do pó com compactação a frio. In Proceedings of the 72nd ABM Annual Congress, São Paulo, Brazil, 2–6 October 2017; Volume 72, pp. 2553–2560.
21. Swain, K.A.; Bahadur, D. Enhanced Stability of Reduced Graphene Oxide Colloid Using Cross-Linking Polymers. *J. Phys. Chem. C* **2014**, *118*, 9450–9457.

22. Yue, H.; Yao, L.; Gao, X.; Zhang, S.; Guo, E.; Zhang, H.; Lin, X.; Wang, B. Effect of ball-milling and graphene contents on mechanical properties and fracture mechanisms of graphene nanosheets reinforced copper matrix composites. *J. Alloys Compd.* **2017**, *691*, 755–762.
23. Gao, X.; Yue, H.; Guo, E.; Zhang, H.; Lin, X.; Yao, L.; Wang, B. Mechanical properties and thermal conductivity of graphene reinforced copper matrix composites. *Powder Technol.* **2016**, *301*, 601–607.
24. Ferrari, A.C.; Basko, D.M. Raman spectroscopy as a versatile tool for studying the properties of graphene. *Nat. Nanotechnol.* **2013**, *8*, 235–246.
25. Pruna, A.; Pullini, D.; Busquets, D. Influence of synthesis conditions on properties of green-reduced graphene oxide. *J. Nanoparticle Res.* **2013**, *15*, 1605.
26. COROS, M.; Pogacean, F.; Turza, A.; Dan, M.; Berghian-Grosan, C.; Pana, I.-O.; Pruneanu, S. Green synthesis, characterization and potential application of reduced graphene oxide. *Phys. E Low-Dimens. Syst. Nanostruct.* **2020**, *119*, 113971.
27. Ghadim, E.E.; Rashidi, N.; Kimiagar, S.; Akhavan, O.; Manouchehri, F.; Ghaderi, E. Pulsed laser irradiation for environment friendly reduction of graphene oxide suspensions. *Appl. Surf. Sci.* **2014**, *301*, 183–188.
28. Loryuenyong, V.; Totepvimarn, K.; Eimburanaprat, P.; Boonchompoo, W.; Buasri, A. Preparation and characterization of reduced graphene oxide sheets via water-based exfoliation and reduction methods. *Ann. Mater. Sci. Eng.* **2013**, *352*, 403–411.
29. Sarkar, C.; Dolui, S.K. Synthesis of copper oxide/reduced graphene oxide nanocomposite and its enhanced catalytic activity towards reduction of 4- nitrophenol *RSC Adv.* **2015**, *5*, 60–72.
30. Zhang, L.; Yang, L.; Zhang, F.; Wang, Y.; Chen, J. In Situ synthesis of three-dimensional graphene skeleton copper azide with tunable sensitivity performance. *Mater. Lett.* **2020**, *279*, 128466.